

Intra- and intertube tunneling transport in ropes of single-walled carbon nanotubes

Cite as: Appl. Phys. Lett. **90**, 232109 (2007); <https://doi.org/10.1063/1.2746963>
 Submitted: 08 March 2007 • Accepted: 14 May 2007 • Published Online: 06 June 2007

K. M. Seemann, J. Ebbecke, A. L. Hörner, et al.



ARTICLES YOU MAY BE INTERESTED IN

[InAsSb / GaSb heterostructure based mid-wavelength-infrared detector for high temperature operation](#)

Applied Physics Letters **90**, 232106 (2007); <https://doi.org/10.1063/1.2746951>

[Highly sensitive sensors for alkali metal ions based on complementary-metal-oxide-semiconductor-compatible silicon nanowires](#)

Applied Physics Letters **90**, 233903 (2007); <https://doi.org/10.1063/1.2746962>

[Electrical and thermal transport properties of magnetically aligned single wall carbon nanotube films](#)

Applied Physics Letters **77**, 666 (2000); <https://doi.org/10.1063/1.127079>

 QBLOX



1 qubit

Shorten Setup Time
Auto-Calibration
More Qubits

Fully-integrated
Quantum Control Stacks
Ultrastable DC to 18.5 GHz
 Synchronized <<1 ns
 Ultralow noise



100s qubits

[visit our website >](#)



Intra- and intertube tunneling transport in ropes of single-walled carbon nanotubes

K. M. Seemann,^{a)} J. Ebbecke, A. L. Hörner, and A. Wixforth

Institut für Physik der Universität Augsburg, Universitätsstrasse 1, D-86159 Augsburg, Germany

(Received 8 March 2007; accepted 14 May 2007; published online 6 June 2007)

The authors report on intra- and intertube tunneling induced current oscillations in an individual rope of single-walled carbon nanotubes. Defects within single tubes and tube-tube contacts provide tunneling barriers of different transparencies and heights, respectively, and the formation of quantum dots in between. As a function of the bias voltage, the authors observe a transition from an intratube to an intertube tunneling dominated transport. The samples were fabricated on prepatterned silicon substrates employing surface acoustic wave induced streaming leading to an alignment of the ropes with respect to the contacts. © 2007 American Institute of Physics.

[DOI: 10.1063/1.2746963]

The quasi-one-dimensional molecular structure of carbon nanotubes¹ (CNTs) reveals many interesting physical phenomena ranging from mechanical over electronic to optical peculiarities.^{2–4} Over the last few years, apart from many other applications, CNT have been also considered as building blocks of future electronic systems. This is partially triggered by the fact that they exhibit either a semiconducting or a metallic behavior depending on their molecular structure. A further dimensional reduction from a one dimensional behavior towards a quasi-zero-dimensional quantum dot can be realized by the deposition of CNT between two metal electrodes. Ideally, CNT devices consist of individual single-walled CNTs (SWCNTs) with clearly defined electronic properties. More realistically, one has to deal with ropes of carbon nanotubes (RCNTs), consisting of metallic and semiconducting single-walled CNTs. In a rope of carbon nanotubes one typically has to consider both metallic and semiconducting tubes, with different chiralities, lengths, and defect densities. Here, we report on our experimental investigation of such CNT ropes. We employ surface acoustic waves to deposit and align CNT from an aqueous suspension^{5–8} onto a prepatterned silicon chip.

For the experiments reported here, a purified SWCNT raw material was purchased from Tubes@Rice, Houston, USA. The silicon chip of $5 \times 5 \text{ mm}^2$ was cut from an As doped n^+ substrate of $0.001\text{--}0.005 \text{ } \Omega \text{ cm}$ resistivity and $\langle 001 \rangle$ orientation. A 200 nm thick SiO_2 layer, deposited in a plasma enhanced chemical vapor deposition process serves as a gate dielectric for a back gate contact. Electron beam lithography (eline©) was used to pattern 18 contact pairs. A CNT junction fabricated using this method is shown in Fig. 1(a). In order to determine their morphology, the CNT have been characterized by transmission electron microscopy (TEM) prior to deposition. These studies revealed rope structures with diameters of approximately 5–10 nm, as depicted in Fig. 1(b). A compositionally disordered rope thus represents a more complicated electronic system than an individual metallic or semiconducting SWCNT. Our single rope samples have been characterized by two-terminal I - V measurements with a gate bias as a parameter at low temperatures. The gate voltage was applied to the back gate contact

of the n^+ silicon substrate, as shown in the inset in Fig. 1 and separated from the RCNT by the 200 nm thick SiO_2 insulating layer directly on top of the n^+ substrate. The two-terminal resistance at room temperature is $R=54 \text{ M}\Omega$. With decreasing temperature, the I - V curves become non-linear with the typical signatures of a tunneling barrier forming between the RCNT and the metal contacts. Figure 2 shows the I - V characteristics measured at $T=1.5 \text{ K}$ for different gate voltages

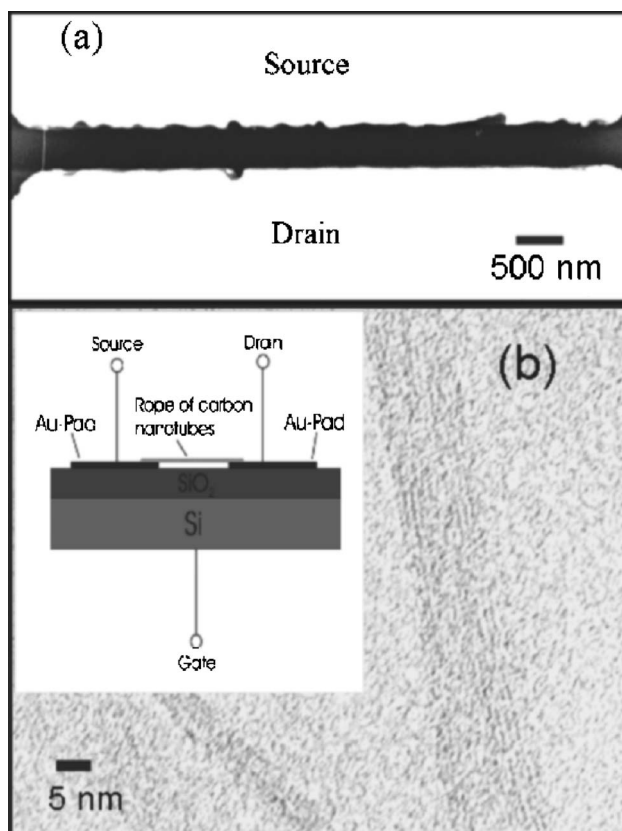


FIG. 1. (a) Scanning electron microscopy image of a carbon nanotube junction based on a rope of single-walled carbon nanotubes. The carbon nanotube rope has a diameter of 5 nm. (b) Transmission electron microscopy image of several ropes of single-walled carbon nanotubes. The substructure of each carbon nanotube rope clearly reveals several individual single-walled carbon nanotubes adhering to each other and forming a rope structure. The inset shows the schematic sample layout.

^{a)}Electronic mail: phyks@leeds.ac.uk

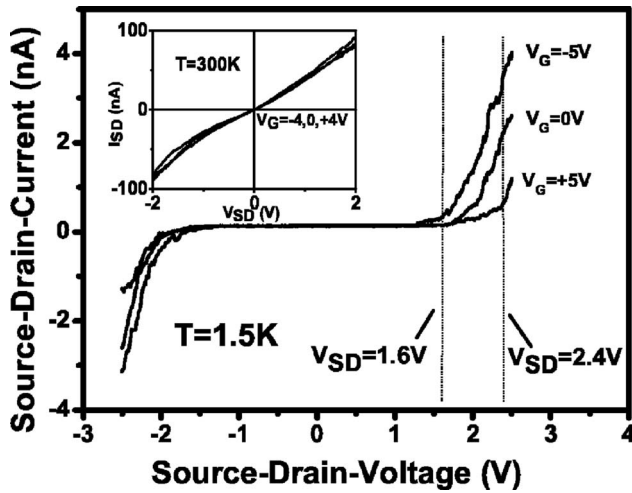


FIG. 2. I - V characteristics of a carbon nanotube junction measured at $T = 300$ K (inset) and $T = 1.5$ K for various gate voltages. The effective tunneling barrier energy for the nonbiased gate is approximately $U_{\text{barrier}} = 1.9$ eV, which can be increased or decreased by applying a negative or a positive gate voltage, respectively. Different gate voltages also have an effect on the differential conductance at $V_{\text{source-drain}} = 2.4$ V.

$V_{\text{gate}} = +5, 0,$ and -5 V. At $T = 1.5$ K the field effect response of the carbon nanotube junction yields for $V_{\text{source-drain}} = 2$ V a value of $I_{\text{source-drain}}/V_{\text{gate}} = 0.2$ nA/V. Thus, we classify the compositionally disordered RCNT to be dominated by transport through metallic SWNTs with a weak semiconducting component of a narrow band gap.

In the conducting regime, i.e., for a source-drain bias above $V_{\text{source-drain}} \approx 1.5$ V, we observe strongly fluctuating and aperiodic, yet highly reproducible $I(V_{\text{gate}})$ characteristics. Moreover, the two-terminal I - V_{gate} measurements at $V_{\text{source-drain}} = 1.6$ V and $T = 1.5$ K, just below the threshold of the effective tunneling barrier energy $U_{\text{barrier}} = 1.9$ eV, exhibit an aperiodic sequence of conductance peaks of different heights, as shown in Fig. 3. We attribute these current peaks to be of Coulomb blockade nature.

The aperiodic sequence of current peaks points out the formation of multiple quantum dots within the RCNT connected in series.^{9,10} Current peaks appear only at those gate voltages where the Coulomb blockade of all quantum dots is suppressed. The multiple quantum dots are populated and depopulated via the tunneling contacts at the Au-RCNT interface and are a typical feature of a junction consisting of an individual RCNT bridging two tunneling contacts. Additionally, we observed current oscillations in the RCNT junction at a bias voltage of $V_{\text{source-drain}} = 2.4$ V, significantly above the effective tunneling barrier energy $U_{\text{barrier}}(1.5$ K). These are aperiodic as well but differ, however, both in peak spacing and width, from those measured at $V_{\text{source-drain}} = 1.6$ V. At a bias of $V_{\text{source-drain}} = 1.6$ V, sharply separated current peaks are measured, as shown in the inset in Fig. 3. On the other hand, at a bias voltage of $V_{\text{source-drain}} = 2.4$ V, well above the effective tunneling barrier energy U_{barrier} , the separated peaks in the current response remain persistent, as can be seen in Fig. 3. Again, these current oscillations were highly reproducible.

We additionally find a positive linear current response superimposed to our I - V_{gate} curve manifesting a V-shaped current characteristic. This enhanced conductivity of the CNT junction at higher positive and negative gate voltages is based on the increasing differential conductance of the

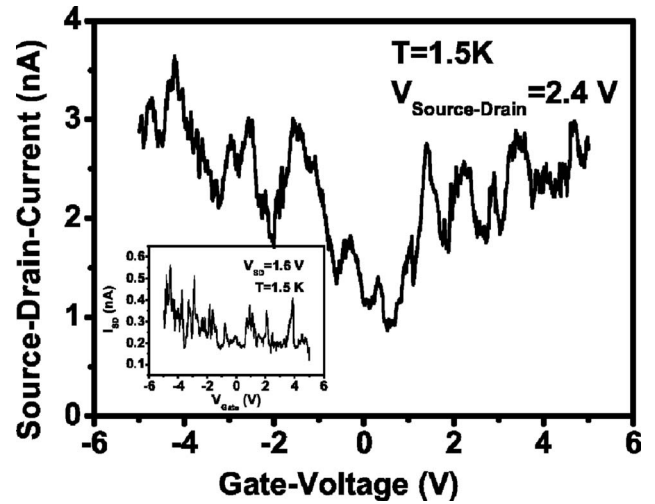


FIG. 3. Source-drain current as a function of the gate voltage measured at $T = 1.5$ K and at a source-drain voltage of $V_{\text{source-drain}} = 2.4$ V being well above the effective tunneling barrier height formed at the carbon nanotube-metal pad interface. A peak broadening to typically $\Delta V_{\text{gate}} = 1.0$ V appears besides approximately tenfold current values compared to the case at $V_{\text{source-drain}} = 1.6$ V. The V-shaped characteristic is a fingerprint of the enhanced differential conductance at nonzero gate voltages. Inset: source-drain current as a function of the gate voltage measured at $T = 1.5$ K for a source-drain voltage of $V_{\text{source-drain}} = 1.6$ V, just below the zero-bias tunneling barrier height.

RCNT compared to the case of an unbiased gate, which leads to an improved transparency of the tunneling barrier at the metal pad-RCNT interface.

To further understand the nature of the persistent high bias current oscillations, we calculate the energy level spacing of the quantum dots within our RCNT from their measured distance on the gate voltage scale and from $\Delta E = \Delta V_G \cdot e \cdot C_G / C_T - e^2 / C_T$ in the low bias voltage case (i.e., $V_{\text{source-drain}} = 1.6$ V) and the high bias voltage case ($V_{\text{source-drain}} = 2.4$ V).¹¹ Here, ΔV_G is a current peak distance taken from our I - V_{gate} curves [Fig. 3 and inset], while C_T is the total electrostatic capacitance of the CNT junction and C_G denotes the electrostatic capacitance between CNT and gate electrode. We calculated the capacitances from $C \approx 2\pi\epsilon_0 L / \ln(2L/d)$ (Ref. 12) and obtained a capacitance of 20 aF for the $L \approx 3$ μm long part of the rope attached to the source and drain contact pads and a capacitance value of $C_G \approx 4$ aF for the part of the CNT rope associated with the source-drain gap of $L = 0.5$ μm . From this, we evaluate the energy level spacing ΔE_{MSQD} of the serial multiple quantum dot chain within the RCNT to be in the range of $\Delta E_{\text{MSQD}} = 10$ –110 meV (inset in Fig. 3). In comparison, we calculate the energy level spacing of the complete RCNT ΔE_{RCNT} to be in the range of $\Delta E_{\text{RCNT}} = 70$ –250 meV for peak distances determined from the measurement shown in Fig. 3. A direct comparison of the energy level spacing for both bias voltage cases is shown in Fig. 4.

Recent theoretical studies¹³ on the electronic properties of carbon nanotube ropes explain the aperiodic set of oscillations that occur in parallel with the ones just discussed once we apply a source-drain bias voltage of $eV_{\text{source-drain}} = 2.4$ eV $> U_{\text{barrier}}(1.5$ K). From our TEM investigations of the RCNT, we have reason to assume that it is comprised of approximately ten individual parallel SWCNTs adding up to a rope of $d = 5$ nm diameter. Maarouf *et al.*¹³ have calculated the energy scales dominating the intertube

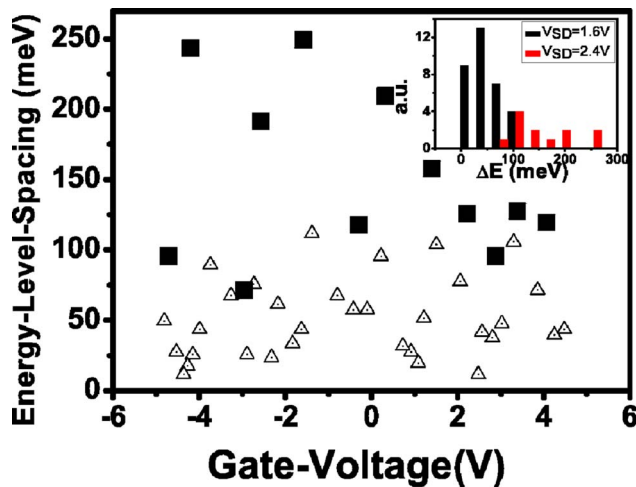


FIG. 4. (Color online) Energy level spacing ΔE vs gate bias voltage V_{gate} . The energy level spacing increases visibly with the source-drain bias voltage changing from $V_{\text{source-drain}}=1.6$ V (open triangles) to $V_{\text{source-drain}}=2.4$ V (filled boxes). The inset shows a histogram of the energy level spacing before and after applying a high source-drain bias voltage.

coupling in a rope of carbon nanotubes. They calculated the energy mismatch between bands of adjacent tubes depending in the helical angles in the vicinity of the Fermi points to be of the order of $\Delta\epsilon \approx 300$ meV. Surpassing this energy mismatch by means of increasing the source-drain bias voltage as we do in our RCNT junction enables strong intertube coupling processes to occur within the RCNT junction, as the condition $eV_{\text{source-drain}} - U_{\text{barrier}}(1.5 \text{ K}) > \Delta\epsilon$ is met at $V_{\text{source-drain}}=2.4$ V. With the intratube tunneling barrier energy $U_{\text{IT-barrier}}$ being much lower than the intertube tunneling barrier $U_{\text{TT-barrier}}$, $U_{\text{IT-barrier}} \ll U_{\text{TT-barrier}}$, and $U_{\text{TT-barrier}} \approx 300$ meV,¹³ intertube electron tunneling occurs once the applied source-drain voltage surpasses the effective tunneling barrier between tube and contact pad and the intertube tunneling barrier as well, $eV_{\text{source-drain}} > U_{\text{barrier}} + U_{\text{TT-barrier}}$. The observation of a clear enhancement of the energy level spacing in our I - V curves is hence a strong indication that we have to contemplate two differently confined quantum dot systems within the CNT rope.

In conclusion, we have observed simultaneous tunneling through both defect induced and intertube tunneling barrier induced multiple quantum dots within a rope of carbon nanotubes. From our experimental findings, we conclude that a rope of carbon nanotubes represents a complex network of quantum conductors, best described by a compositional disordered rope, which consists of metallic nanotubes, possibly embedded in a semiconducting matrix.

The authors thank Udo Beierlein for support with the SWCNTs and for helpful discussions. Financial support from the Bayerische Forschungsstiftung (Fornano) and the Deutsche Forschungsgemeinschaft (SFB 486) is gratefully acknowledged. This research of our group is also supported in part by the German government through the Cluster of Excellence "NIM."

¹S. Iijima, *Nature (London)* **354**, 56 (1991).

²*Carbon Nanotubes: Synthesis, Structure Properties and Applications*, Topics in Applied Physics Vol. 80, edited by M. S. Dresselhaus, G. Dresselhaus, and P. Avouris (Springer-Verlag, Berlin, 2001), Vol. 80, p. 152.

³S. Reich, C. Thomsen, and J. Maultzsch, *Carbon Nanotubes* (Wiley-VCH, Weinheim, 2003).

⁴J. Ebbecke, C. J. Strobl, and A. Wixforth, *Phys. Rev. B* **70**, 233401 (2004).

⁵C. J. Strobl, C. Schaefflein, U. Beierlein, J. Ebbecke, and A. Wixforth, *Appl. Phys. Lett.* **85**, 1427 (2004).

⁶J. M. Bonard, T. Stora, J. P. Salvetat, F. Maier, T. Steckli, C. Duschl, L. Forró, W. A. de Heer, and A. Châtelain, *Adv. Mater. (Weinheim, Ger.)* **9**, 827 (1997).

⁷M. J. O'Connell, S. M. Bachilo, C. B. Huffmann, V. C. Moore, M. S. Strano, E. H. Haroz, K. L. Rialon, P. J. Boul, W. H. Noon, C. Kittrell, J. P. Ma, R. H. Hauge, R. B. Weisman, and R. E. Smalley, *Science* **297**, 593 (2002).

⁸K. M. Seemann, J. Ebbecke, and A. Wixforth, *Nanotechnology* **17**, 4529 (2006).

⁹I. M. Ruzin, V. Chandrasekhar, E. I. Levin, and L. I. Glazman, *Phys. Rev. B* **45**, 13469 (1992).

¹⁰S. Moriyama, K. Toratani, D. Tsuya, M. Susuki, Y. Aoyagi, and K. Ishibashi, *Physica E (Amsterdam)* **24**, 46 (2004).

¹¹L. P. Kouwenhoven, C. M. Marcus, P. L. McEuen, S. Tarucha, R. M. Westervelt, and N. S. Wingreen, *Advanced Study Institute on Mesoscopic Electron Transport* (Kluwer, New York, 1997), Vol. 1, p. 14.

¹²A. Bezryadin, A. R. M. Verschueren, S. J. Tans, and C. Dekker, *Phys. Rev. Lett.* **80**, 4036 (1998).

¹³A. A. Maarouf, C. L. Kane, and E. J. Mele, *Phys. Rev. B* **61**, 11156 (2000).